

## Salinity Intrusion in Estuaries

D. PRANDLE

*Institute of Oceanographic Sciences, Bidston Observatory, Merseyside, England L43 7RA*

(Manuscript received 17 February 1981, in final form 27 July 1981)

### ABSTRACT

One dimensional time-averaged solutions are examined for salinity intrusion in estuaries with a breadth variation  $B_L(X/\lambda)^m$  and a depth variation  $H(X/\lambda)^n$ , where  $X$  is the distance from the head of the estuary. These solutions emphasize the importance of the rate of change of cross-sectional area in determining salinity distribution.

Assuming a constant longitudinal-dispersion coefficient  $D_x = D$ , the salinity distribution is shown to be highly dependent on the dimensionless parameter  $V' = U_1 \times X_1/D$ , with  $U_1$  the velocity of the fresh-water flow at position  $X_1$ , where the estuary is effectively at oceanic salinity. [This parameter  $V'$  is equivalent to the flushing number  $F$  introduced by Arons and Stommel (1951) for the case of an estuary of rectangular cross section.] For eight estuaries, comparisons are made between calculated and observed salinity distributions, where for each estuary the value of  $D$  in the calculated distribution was chosen to produce the best agreement with the observed distribution. For six of the eight estuaries, the chosen value of  $D$  was within the range  $50 \text{ m}^2 \text{ s}^{-1} < D < 500 \text{ m}^2 \text{ s}^{-1}$ , in good agreement with corresponding values found in previous studies. However, it is shown that the salinity distribution is highly sensitive to the specified value of  $D$ , implying that the usefulness of the one-dimensional, time-averaged solutions may be somewhat restricted.

Theoretical distributions of salinity also were obtained for  $D_x = D_1 dc/dx$  and  $D_x = D_2 (dc/dx)^2$ , where  $dc/dx$  represents the time-averaged longitudinal salinity gradient and  $D_1$  and  $D_2$  are constant coefficients. While reasonable agreement is again obtained with observed distributions, certain limitations in the application of these two forms for  $D_x$  are shown.

Attempts to derive a more rational dimensionless form for  $D_x$  in terms of gross estuarine parameters proved unsuccessful.

### 1. Introduction

In a previous paper, Prandle and Rahman (1980) calculated tidal responses in estuaries described by the following geometry

for depth

$$H(X) = H_L(X/\lambda)^m, \quad (1)$$

and

for breadth

$$B(X) = B_L(X/\lambda)^n, \quad (2)$$

where  $X$  is the distance measured from the head;  $\lambda = \sqrt{gH_L}P$  with  $g$  the acceleration due to gravity and  $P$  the tidal period;  $H_L$ ,  $B_L$ ,  $m$  and  $n$  are parameters which relate (1) and (2) to the actual estuarine geometry. The tidal response was expressed analytically in terms of the distance along the estuary and an "estuarine shape number"  $\nu = (n+1)/(2-m)$ . A classification system for estuaries was established against which the behavior of any particular estuary [approximating Eqs. (1) and (2)] could be interpreted. The present paper seeks to extend this approach to consider saline intrusion in es-

tuaries; a basic review of this problem was given by Holley and Harleman (1965).

One immediate difficulty in this extension is that, while tidal propagation in estuaries can be reasonably well described by linearized one-dimensional equations, the physical description of saline intrusion tends to be much more complex (Fischer, 1976). Fischer *et al.* (1979, Chap. 7) state that one-dimensional mixing models may be acceptable providing the estuary is not significantly stratified and that cross-sectional mixing is sufficiently rapid.

A major difficulty in the one-dimensional approach is that all dispersive processes must be represented by a single longitudinal-dispersion coefficient  $D_x$ , whereas physically it is well recognized (Harleman and Ippen, 1967) that vertical dispersion predominates [or, in some instances, lateral circulation (Fischer, 1972)]. Clearly then, the magnitude of the longitudinal dispersion coefficient cannot be easily defined (Smith, 1976, 1980; Holley, *et al.* 1970). Some studies have assumed a constant value for  $D_x$ , others have used values of  $D_x$  related to the concentration gradient along the estuary. Thus, an important objective here is to examine for a range of estuarine conditions (i) the appropriate form and

value for  $D_x$  and (ii) the sensitivity of the salinity distribution to the prescribed value of  $D_x$ . To this end, the analytical solutions of the time-averaged mixing equation are obtained for three separate assumed forms for  $D_x$ . Using in the main, a dimensionless approach, the salinity distributions described by these analytical solutions are evaluated by comparison with observed distributions in eight estuaries.

It should be emphasized that the present paper does not aim to promote the use of one-dimensional estuarine mixing models. The limitations of such models, particularly in the time-averaged mode, are well recognized. However, since such models have been widely used in the past (e.g., Kent, 1960; Williams, and West, 1973) and continue to be used (Curran, 1981), it is of interest to understand some of their characteristics and particularly their dependency on the form of the dispersion coefficient. In addition, the present paper seeks to use this one-dimensional approach to establish some relationship between estuarine shape and the degree of saline intrusion.

**2. Equations of motion and mass conservation**

Tidal propagation in a narrow channel of rectangular cross section may be approximated by the following linearized equations (Ippen, 1966, Chap. 10):

Motion along the  $\chi$  axis

$$\frac{\partial U}{\partial T} + g \frac{\partial Z}{\partial X} + SU = 0, \tag{3}$$

continuity,

$$\frac{\partial Z}{\partial T} + \frac{1}{B} \frac{\partial}{\partial X} (BHU) = 0 \tag{4}$$

and for mass-conservation (Ippen, 1966, Chap. 14)

$$\frac{\partial c}{\partial T} + U \frac{\partial c}{\partial X} = \frac{1}{A} \frac{\partial}{\partial X} \left( AD_x \frac{\partial c}{\partial X} \right), \tag{5}$$

where

- $U$  velocity along the  $X$  axis
- $Z$  elevation above a horizontal datum
- $g$  acceleration due to gravity,
- $S$  linearized friction coefficient
- $B$  channel breadth
- $H$  channel depth
- $A$  cross-sectional area ( $=BH$ )
- $T$  time
- $c$  relative concentration of any conservative substance (dimensionless)
- $D_x$  longitudinal dispersion coefficient.

In order to convert Eqs. (1)–(5) to dimensionless form we introduce the tidal period  $P$  as the unit of time,  $\lambda$  as the unit of horizontal dimension and  $H_L$  as the unit of vertical dimension. These parameters are assumed to be related by

$$\lambda = (gH_L)^{1/2}P. \tag{6}$$

Thus, we obtain the dimensionless variables

$$\begin{aligned} x &= X/\lambda, \quad t = T/P, \quad z = Z/H_L, \quad s = SP \\ b &= B/\lambda, \quad b_L = B_L/\lambda, \quad h = H/H_L, \\ u &= U(P/\lambda) \quad \text{and} \quad d_x = D_x(P/\lambda^2). \end{aligned} \tag{7}$$

Eqs. (1)–(5) may then be rewritten as follows:

$$h(x) = x^m, \tag{8}$$

$$b(x) = b_L x^n, \tag{9}$$

$$\frac{\partial u}{\partial t} + \frac{\partial z}{\partial x} + su = 0, \tag{10}$$

$$\frac{\partial z}{\partial t} + \frac{1}{x^n} \frac{\partial}{\partial x} (ux^{m+n}) = 0. \tag{11}$$

$$\frac{\partial c}{\partial t} + u \frac{\partial c}{\partial x} = \frac{1}{x^{m+n}} \frac{\partial}{\partial x} \left( d_x x^{m+n} \frac{\partial c}{\partial x} \right). \tag{12}$$

In the case of an estuary subjected to tidal forcing at the frequency  $\omega (=2\pi/p)$  we seek solutions of the form

$$z(x, t) = \bar{z}(x) + z'(x)e^{i\omega t}, \tag{13}$$

$$u(x, t) = \bar{u}(x) + u'(x)e^{i\omega t}, \tag{14}$$

and

$$c(x, t) = \bar{c}(x) + c'(x)e^{i\omega t}, \tag{15}$$

where the overbar indicates the time-averaged value and the prime the complex amplitude (representing real amplitude and phase) of the oscillatory component.

Substituting (13), (14) and (15) into (10), (11) and (12) and then resolving the resultant equations into a time-invariant component and a component at the frequency  $\omega$ , we obtain the following time-averaged equations:

$$\frac{\partial}{\partial x} \bar{z} + s\bar{u} = 0, \tag{16}$$

$$\frac{\partial}{\partial x} (\bar{u}x^{m+n}) = 0, \tag{17}$$

$$\bar{u} \frac{\partial \bar{c}}{\partial x} = \frac{1}{x^{m+n}} \frac{\partial}{\partial x} \left( d_x x^{m+n} \frac{\partial \bar{c}}{\partial x} \right). \tag{18}$$

The left-hand side of (18) is subsequently referred to as the advective term and the right-hand side as the dispersive term. For the oscillatory part, first eliminating  $z$  from (10) and (11), we obtain

$$\frac{\partial^2 u}{\partial t^2} + s \frac{\partial u}{\partial t} = \frac{\partial}{\partial x} \left[ \frac{1}{x^n} \frac{\partial}{\partial x} (ux^{m+n}) \right]. \tag{19}$$

Thus for the component of frequency  $\omega$

$$-u'(\omega^2 - i\omega s) = \frac{\partial}{\partial x} \left[ \frac{1}{x^n} \frac{\partial}{\partial x} (u'x^{m+n}) \right]. \tag{20}$$

For the mass-conservation equation, we obtain

$$i\omega c' + \bar{u} \frac{\partial c'}{\partial x} + \mathbf{u}' \frac{\partial \bar{c}}{\partial x} = \frac{1}{x^{m+n}} \frac{\partial}{\partial x} \left[ \partial_x x^{m+n} \frac{\partial c'}{\partial x} \right]. \quad (21)$$

Solutions for  $\mathbf{u}'$  and  $\mathbf{z}'$  were obtained by Prandle and Rahman (1980) both for the case of an estuary with the head at  $x = 0$  and for an estuary closed by a barrier at any intermediate position  $x = a$ . A corresponding analytical solution of (21) cannot be obtained, and subsequent interest here will be confined to the time-averaged solutions from Eqs. (16)–(18).

### 3. Time-averaged solutions

In a time-averaged solution, the duration of the averaging period should normally exceed the longest cyclical variation. However, in the present application the objective in time-averaging is to filter the predominant tidal oscillations, and hence the averaging period is one semidiurnal tide (or diurnal where appropriate). Thus longer term variations in freshwater flow require a series of separate solutions each with varying values of  $Q$ . Unfortunately, successive semidiurnal tides are not identical but generally vary over a 15-day spring-neap cycle. Some account of these longer term tidal variations might be incorporated by some adjustment of  $Q$  so that, for example, increased upstream storage during the time of increasing tidal ranges might be compensated by decreasing  $Q$ . These complications in applying the time-varying solutions pose serious difficulties in the later comparison of observed and theoretical salinity distributions (Section 4).

Since we now only consider time-averaged values of  $U$ ,  $Z$  and  $C$  it is convenient to drop the overbar. Integrating (17) gives

$$ux^{m+n} = q/b_L, \quad (22)$$

where  $q$  is a constant which may be compared with the freshwater flow  $Q$ , where

$$Q = UBH = \left( u \frac{\lambda}{P} \right) B_L H_L x^{m+n} = q \frac{\lambda^2 H_L}{P}. \quad (23)$$

Substituting (22) into (16), we obtain

$$\frac{dz}{dx} = \frac{-sq}{b_L x^{m+n}}. \quad (24)$$

This demonstrates that mean sea level rises toward the head ( $x = 0$ ) of an estuary with the rise increasing as 1) the freshwater flow increases, 2)  $m + n$  increases (i.e., a more rapidly truncating estuary) and 3)  $x$  decreases. Strictly, (24) should include contributions due to the longitudinal density gradient

and the tidal ‘‘radiation stress’’ (Nihoul and Roday, 1975); these terms can be omitted on scaling grounds in (3) but after time averaging they may be of the same order as the surface gradient.

Substituting (22) into (18) gives

$$\frac{q}{b_L} \frac{dc}{dx} = \frac{d}{dx} \left( d_x x^{m+n} \frac{dc}{dx} \right). \quad (25)$$

Integrating (25),

$$\frac{q}{b_L} c = d_x x^{m+n} \frac{dc}{dx} + \text{constant } (K). \quad (26)$$

We now introduce upstream and downstream boundary conditions. The upstream condition is defined as the position  $x = a$  at the limit of saltwater intrusion, where the water is entirely fresh, i.e.,  $C = 0$ . The downstream condition is defined as the position  $x = x_1$ , where the influence of freshwater flow is negligible and  $C = C_1$  is the oceanic salinity. Thus, in summary

$$\begin{aligned} \text{at some downstream position } x = x_1, \quad c = c_1 \\ \text{at some upstream position } x = 0, \quad c = 0. \end{aligned} \quad (27)$$

Three solutions are presented corresponding to the following values for

$$(i) \quad d_x = d; \quad \text{or in dimensional form } D_x = D, \quad (28)$$

$$(ii) \quad d_x = d_1 \frac{dc}{dx}; \quad \text{or } D_x = D_1 \frac{dc}{dx}, \quad (29)$$

and

$$(iii) \quad dx = d_2 \left( \frac{dc}{dx} \right)^2; \quad \text{or } D_x = D_2 \left( \frac{dc}{dx} \right)^2, \quad (30)$$

where  $d$ ,  $d_1$  and  $d_2$  are constants and  $D = d(\lambda^2/P)$ ,  $D_1 = d_1 \lambda^2/P$ ,  $D_2 = d_2(\lambda^2/P)$  from (7). The latter two forms for  $d_x$  were selected on the basis of similar approximations suggested by Thatcher and Harleman (1972) and Uncles and Radford (1980).

#### a. $d_x$ constant

Substituting (28) into (26), we obtain the following solution satisfying the boundary conditions (27)

$$\frac{c(x)}{c_1} = \frac{\exp \left[ V \left( \frac{x}{x_1} \right)^{1-m-n} \right] - \exp \left[ V \left( \frac{a}{x_1} \right)^{1-m-n} \right]}{\exp V - \exp \left[ V \left( \frac{a}{x_1} \right)^{1-m-n} \right]}, \quad (31)$$

where

$$V = \frac{q}{b_L d} \frac{x_1^{1-m-n}}{(1-m-n)}, \quad (32)$$

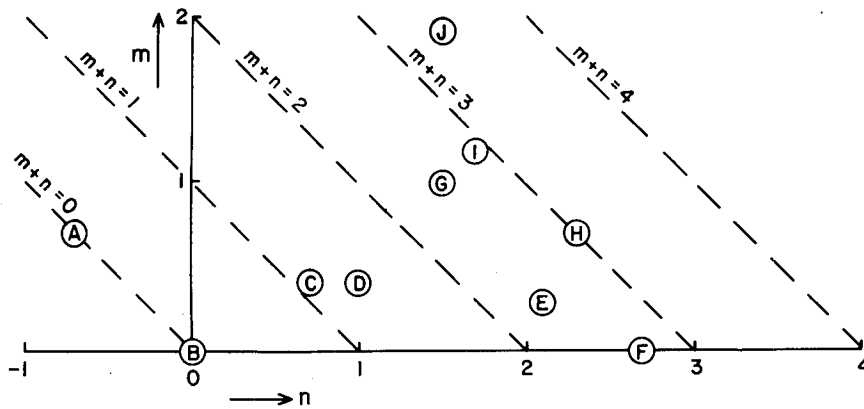


FIG. 1. Values for  $m + n$  for 10 estuaries. A—Fraser; B—Rotterdam Waterway; C—Hudson; D—Potomac; E—Delaware; F—Miramichi; G—Bay of Fundy; H—Thames; I—Bristol Channel; J—St. Lawrence.

or from (22)

$$V = \frac{u_1 x_1}{d(1 - m - n)}, \tag{33}$$

where  $u_1$  is the velocity at  $x_1$ .

Fig. 1 shows a plot of the values of  $m$  and  $n$  for the estuaries studied by Prandle and Rahman (1980). The figure shows that all 10 estuaries lie in the range  $0 < m + n < 4$  and hence we select this range for study here.

Fig. 2 shows typical distributions of  $c(x)/c_1$  over the range of values of  $0 < m + n < 4$  with  $V(1 - m - n) = 10, 1$  and  $0.1$  and for  $a/x_1 = 0.001, 0.1$  and  $0.5$ .

Here and elsewhere the case of  $a/x_1 = 0.001$  is taken as representative of an estuary where saline intrusion extends almost to the head; in adopting this value it should be noted that some of the solutions presented may be sensitive to the precise value of  $a/x_1$  as  $a/x_1 \rightarrow 0$ .

The results show that the character of the distribution in any estuary is primarily determined by the parameter  $V'$  given by

$$V' = V(1 - m - n) = \frac{u_1 x_1}{d} = q/b_L x_1^{m+n-1} d \tag{34}$$

or in dimensional parameters

$$V' = \frac{U_1 X_1}{D} = \frac{Q X_1}{B_1 H_1 D}, \tag{35}$$

where  $B_1$  is the breadth and  $H_1$  the depth at the mouth  $X_1$ . This parameter  $V'$  is identical to the parameter  $F$  introduced by Arons and Stommel (1951) and referred to as the flushing number. However, the formula originally cited for  $F$  refers to an estuary of uniform rectangular cross section and incorporates certain unnecessary assumptions regarding the dispersion coefficient  $D$  and the nature of the tidal oscillations. As the value of this parameter

$V'$  decreases over the range 10–0.1, Fig. 2 shows that the mixing of salt and freshwater occurs successively further upstream. Thus we see that  $V'$  decreases and hence mixing occurs closer to the head as: 1) the freshwater flow  $Q$  decreases, 2) the distance from the head to the mouth  $X_1$  decreases, 3) the breadth at the mouth  $B_1$  increases, 4) the depth at the mouth  $H_1$  increases and 5) the longitudinal dispersion coefficient  $D$  increases. However, the above parameters are strongly interrelated and caution must be exercised in drawing generalized conclusions.

The results for  $V' = 10$  show that mixing is confined to the lower half of the estuary and imposing the condition  $c = 0$  at intermediate locations as far as  $0.5x_1$  from the head (as might result from the construction of a tidal barrier) has a negligible effect on the mixing pattern. By contrast, for  $V' = 0.1$  mixing is confined to the upper half of the estuary except when  $m + n < 1.5$ . For  $V' = 1$  and  $0.1$  maximum intrusion occurs for values of  $m + n$  in the range 0.5–1.5. For these latter values of  $V'$ , imposing the condition  $c = 0$  at intermediate locations  $a/x_2 = 0.1$  and  $0.5$  produces significant changes in the salinity distributions.

In general, the impact of specifying a zero-salinity condition at any position,  $a$ , is proportional to the value of the existing concentration at that position. However, this result takes no account of the change in tidal conditions which might accompany the specification of the zero-salinity condition.

Differentiating (31) with respect to  $x$  gives

$$\frac{d}{dx} \frac{c(x)}{c_1} = \frac{q x^{-m-n}}{b_L d} \exp \left[ V \left( \frac{x}{x_1} \right)^{1-m-n} \right] \times \left\{ \exp V - \exp \left[ V \left( \frac{a}{x_1} \right)^{1-m-n} \right] \right\}^{-1} \tag{36}$$

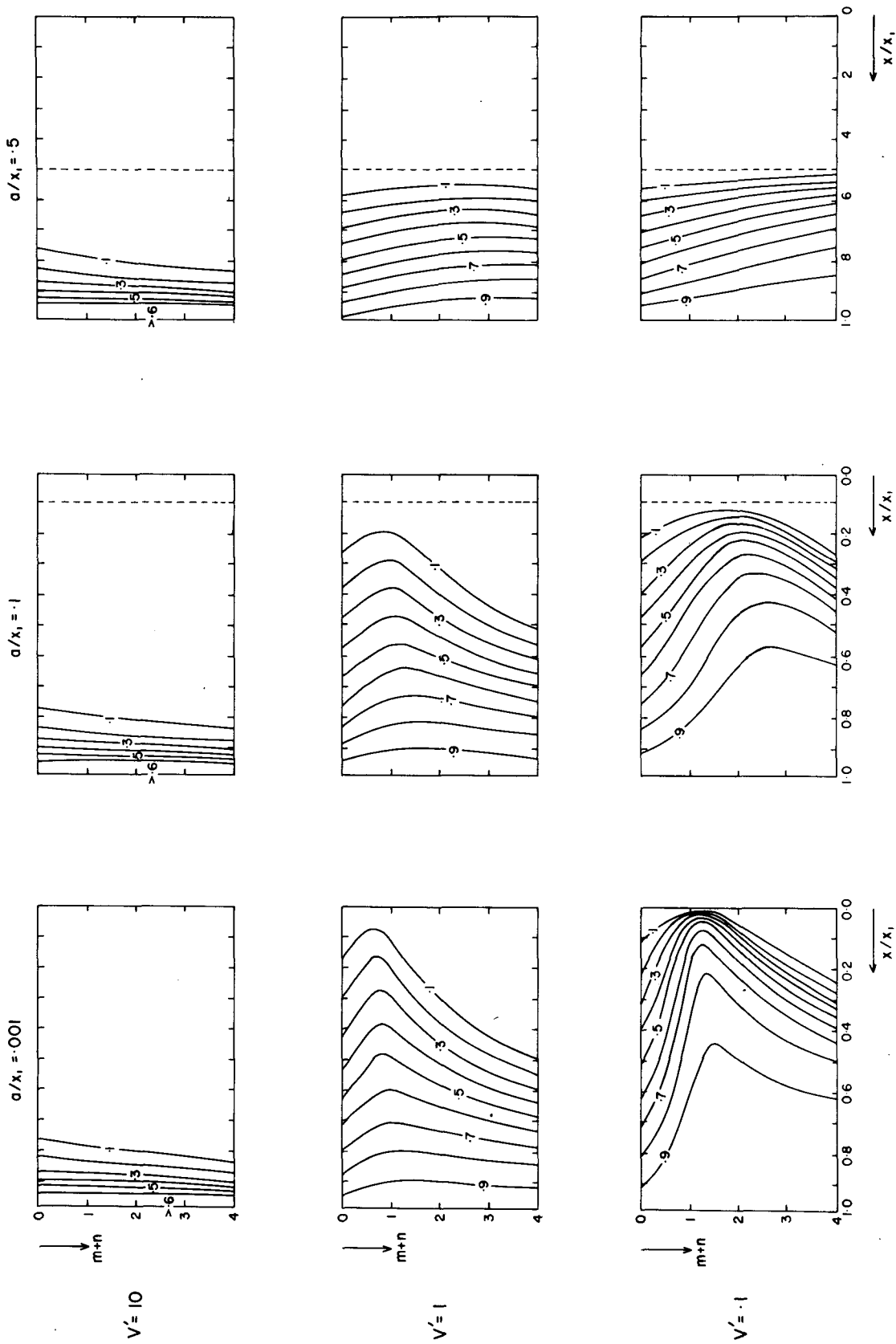


FIG. 2. Plots of  $c(x)/c_1$  for  $d_x = d$  (constant). Contours indicate  $c(x)/c_1$  for  $\alpha/x_1 = 0.001, 0.1$  and  $0.5$  with (a)  $V' = 10$ , (b)  $V' = 1$  and (c)  $V' = 0.1$ .

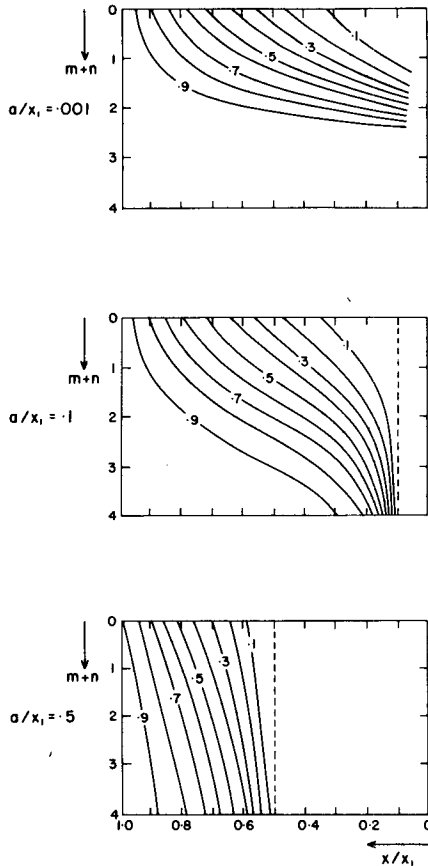


FIG. 3. Plots of  $c(x)/c_1$  for  $d_x = d_1 dc/dx$ . Contours indicate  $c(x)/c_1$  for (a)  $a/x_1 = 0.001$ , (b)  $a/x_1 = 0.1$  and (c)  $a/x_1 = 0.5$ .

and

$$\frac{d^2 c(x)}{dx^2 c_1} = \frac{q}{b_L d} x^{-m-n-1} \left( \frac{q}{b_L d} x^{1-m-n} - m - n \right) \times \exp \left[ V \left( \frac{x}{x_1} \right)^{1-m-n} \right] \times \left\{ \exp V - \exp \left[ V \left( \frac{a}{x_1} \right)^{1-m-n} \right] \right\}^{-1}. \quad (37)$$

Thus, the distributions contain a point of inflection ( $d^2 c/dx^2 = 0$ ) at  $x_{IN}$  given by

$$\frac{x_{IN}}{x_1} = \left( \frac{m+n}{V'} \right)^{1/1-m-n}. \quad (38)$$

In applying the present theory to an estuary for which an observed value of  $x_{IN}$  exists, an appropriate value of  $V'$  may be obtained from (38).

Eq. (31) is indeterminate for the value  $m+n=1$ ; however, for  $m+n=1$  we note the alternative solution for (26) and (27)

$$\frac{c(x)}{c_1} = \frac{\left( \frac{x}{x_1} \right)^{V'} - \left( \frac{a}{x_1} \right)^{V'}}{1 - \left( \frac{a}{x_1} \right)^{V'}}. \quad (39)$$

Eq. (39) clearly illustrates the significance of the parameter  $V'$ . It is also evident that the contribution of the terms involving  $(a/x_1)$  in (39) increases as  $V'$  decreases, confirming the trend noted previously.

b.  $d_x = d_1(dc/dx)$

Substituting (29) into (26), we obtain the following solution satisfying the boundary conditions (27):

$$\frac{c(x)}{c_1} = \frac{\left( \frac{x}{x_1} \right)^{2-n-m} - \left( \frac{a}{x_1} \right)^{2-n-m}}{1 - \left( \frac{a}{x_1} \right)^{2-n-m}} \quad (40)$$

with

$$d_1 = \frac{q}{c_1 b_L} \frac{(x_1^{2-n-m} - a^{2-n-m})}{(2-n-m)^2}. \quad (41)$$

Fig. 3 shows the distribution of  $c(x)/c_1$  given by (40) over the range  $0 < m+n < 4$  for the case of (a)  $a/x_1 = 0.001$ , (b)  $a/x_1 = 0.1$  and (c)  $a/x_1 = 0.5$ . For the case  $a/x_1 = .001$  the figure shows that mixing occurs progressively farther upstream as the parameter  $m+n$  increases.

In this case, the value of  $d_1$  is determined directly by the requirement of satisfying the two boundary conditions and no further adjustment of the resulting distribution is possible. In reality, we might expect the coefficient  $d_1$  to be determined by flow conditions and the value of  $a$ , i.e., the position of zero salinity will vary according to the value of  $d_1$ .

It turns out that by suitably adjusting  $(a/x_1)$ , in most cases the distribution described by (40) can be made to approximate (31) reasonably well. However, by differentiating (40) it can be shown that the agreement between (31) and (40) is limited.

Thus, differentiating (40) with respect to  $x$  gives

$$\frac{d}{dx} \frac{c(x)}{c_1} = (2-n-m) x^{1-n-m} / (x_1^{2-n-m} - a^{2-n-m})$$

and

$$\frac{d^2 c(x)}{dx^2 c_1} = (2-n-m)(1-n-m) x^{-n-m} / (x_1^{2-n-m} - a^{2-n-m}). \quad (42)$$

From which we note that

(i) when  $n+m=1$ ,  $\frac{d^2 c}{dx^2} = 0$ ,  
i.e.  $c$  varies linearly with  $x$ , (43)

(ii) when  $n+m < 1$ ,  $\frac{d^2 c}{dx^2} > 0$ ,  
 $\frac{dc}{dx} = 0$  at  $x = a$ , (44)

(iii) when  $n + m > 1$ ,  $\frac{d^2c}{dx^2} < 0$ ,

$$\frac{dc}{dx} = \infty \text{ at } x = a. \tag{45}$$

These results show important differences from the corresponding results derived in Section 3a. The distribution described by (40) cannot include a point of inflection and the distribution must always be "concave" for  $m + n < 1$  and "convex" for  $m + n > 1$ .

Fig. 4 shows the values of  $d_1$  calculated from (41) for the distributions shown in Fig. 3. The values increase steadily as  $m + n$  increases for  $m + n < 1.5$  but then increase rapidly as  $m + n \rightarrow 2$ . For  $m + n > 2$ ,  $d_1$  is negative and may vary rapidly.

To understand these results for the value of  $d_1$ , we first examine the solution of (26) and (27) for the case of  $m + n = 2$ , i.e., when (40) is indeterminate. Applying L'Hôpital's rule for the limiting case of  $m + n \rightarrow 2$ , (40) reduces to

$$\frac{c(x)}{c_1} = 1 - \frac{\log(x/x_1)}{\log(a/x_1)} \tag{46}$$

and similarly (41) reduces to

$$d_1 = \frac{q}{c_1 b_L} \left( \frac{\log x_1 - \log a}{2(2 - m - n)} \right). \tag{47}$$

Thus, (47) shows that  $d_1 \rightarrow \infty$  as  $m + n \rightarrow 2$ . Expanding the right-hand side (rhs) of (25) for  $m + n = 2$  and substituting (42) for  $dc/dx$  and  $d^2c/dx^2$  we find the rhs goes to zero for finite values of  $d_1$ . Hence to maintain a balance between the advective and dispersive terms in (25) requires an infinite value for  $d_1$ . In the estuarine applications considered here, the dispersion coefficient must be positive and finite and, thus, we conclude that assumption (29) is only valid for estuaries where  $m + n < 2$ . Since (43) shows that  $c$  must vary linearly with  $x$  for  $m + n = 1$  and the "shape" of the distribution is further qualified by (44) and (45) we may further conclude that the range of mixing patterns described by (40) is severely limited.

$$c \cdot dx = d_2 (dc/dx)^2$$

Substituting (30) into (26), we obtain the following solution satisfying the boundary conditions (27):

$$\frac{c(x)}{c_1} = \frac{\left(\frac{x}{x_1}\right)^{(3-n-m)/2} - \left(\frac{a}{x_1}\right)^{(3-n-m)/2}}{1 - \left(\frac{a}{x_1}\right)^{(3-n-m)/2}} \tag{48}$$

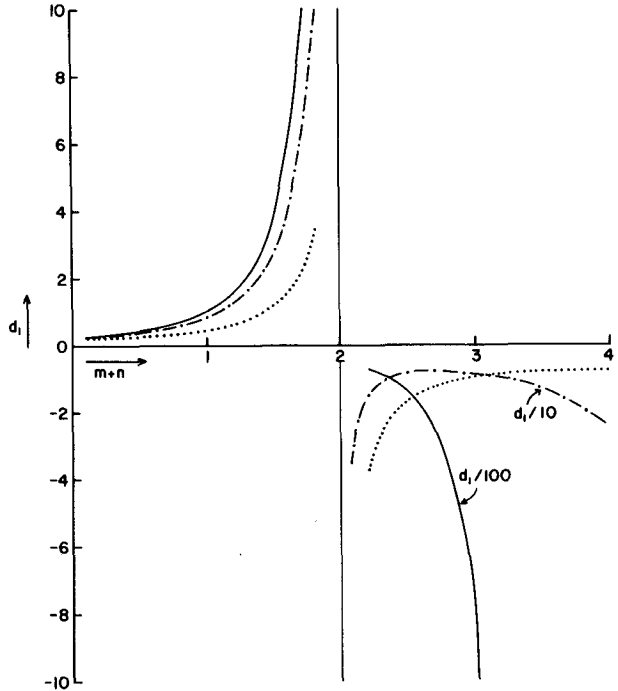


FIG. 4. Plots of  $d_1/(g/c_1 b_L)$  where  $d_x = d_1 dc/dx$ . (—)  $a/x_1 = 0.001$ ; (---)  $a/x_1 = 0.1$ ; (····)  $a/x_1 = 0.5$ .

with

$$d_2 = \frac{q}{c_1^2 b_L} (x_1^{(3-n-m)/2} - a^{(3-n-m)/2}) \times \left( \frac{3-n-m}{2} \right)^{-3}. \tag{49}$$

Fig. 5 shows the distribution of  $c(x)/c_1$  given by (48) over the range  $0 < m + n < 4$  for the case of 1)  $a/x_1 = 0.001$ , 2)  $a/x_1 = 0.1$  and 3)  $a/x_1 = 0.5$ . These distributions are essentially similar to those shown in Fig. 3 for  $d_x = d_1 (dc/dx)$ . When  $n + m = 1$  these two distributions are identical, whereas at higher values of  $n + m$  Eq. (48) extends the mixing zone to a greater part of the estuary than the more confined zone near the head shown by (40).

Differentiating (48) with respect to  $x$  gives

$$\frac{d}{dx} \frac{c(x)}{c_1} = \left( \frac{3-n-m}{2} \right) x^{(1-n-m)/2} \times (x_1^{(3-n-m)/2} - a^{(3-n-m)/2})^{-1}$$

and

$$\frac{d^2}{dx^2} \frac{c(x)}{c_1} = \left( \frac{3-n-m}{2} \right) \left( \frac{1-n-m}{2} \right) x^{(-1-n-m)/2} \times (x_1^{(3-n-m)/2} - a^{(3-n-m)/2})^{-1}. \tag{50}$$

From which we note that

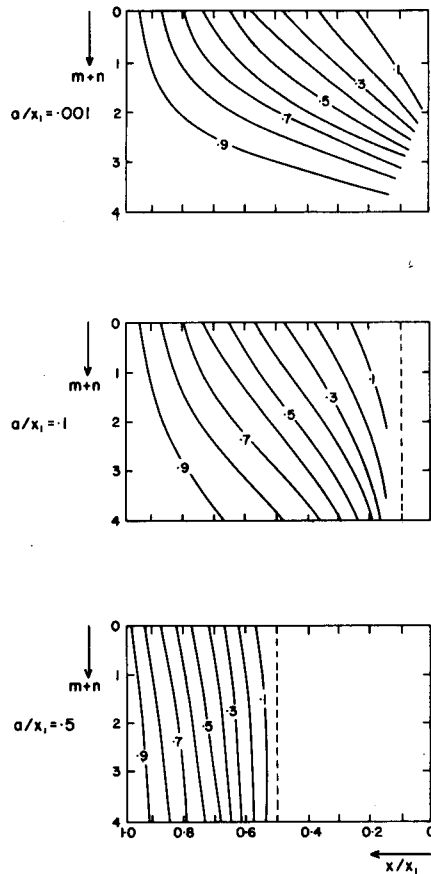


FIG. 5. Plots of  $c(x)/c_1$  for  $d_x = d_2(dc/dx)^2$ . Contours indicate  $c(x)/c_1$  for (a)  $a/x_1 = 0.001$ , (b)  $a/x_1 = 0.1$  and (c)  $a/x_1 = 0.5$ .

(i) when  $n + m = 1$ ,  $\frac{d^2c}{dx^2} = 0$ ,  
 i.e.,  $c$  varies linearly with  $x$ , (51)

(ii) when  $n + m < 1$ ,  $\frac{d^2c}{dx^2} > 0$ ,  
 $\frac{dc}{dx} = 0$  at  $x = a$ , (52)

(iii) when  $n + m > 1$ ,  $\frac{d^2c}{dx^2} < 0$ ,  
 $\frac{dc}{dx} = \infty$  at  $x = a$ . (53)

These results, (51), (52) and (53), are identical to those derived in Section 3b [Eqs. (43), (44) and (45)] and confirm the similarity between the two approximations for  $d_x$ .

Fig. 6 shows the values of  $d_2$  calculated from (49) for the distributions shown in Fig. 5. The values increase progressively with increasing values of  $m + n$  for  $m + n < 2$  but show rapid increases as

$m + n$  approaches 3. For  $m + n > 3$ ,  $d_2$  is negative and may vary rapidly.

In the present case (48) is indeterminate for  $m + n = 3$ . Applying L'Hôpital's rule for the limiting case we find, for  $m + n \rightarrow 3$

$$\frac{c(x)}{c_1} = 1 - \log\left(\frac{x}{x_1}\right) / \log\left(\frac{a}{x_1}\right) \quad (54)$$

and similarly for (49)

$$d_2 = \frac{q}{c_1^2 b_L} \left[ \frac{\log x_1 - \log a_1}{3 \left( \frac{3 - n - m}{2} \right)^2} \right] \quad (55)$$

In view of the similarity between these results and those shown in Section 3b we may conclude that assumption (30) is only valid for estuaries where  $m + n < 3$ . Noting that (54) for  $m + n = 3$  is identical to (46) for  $m + n = 2$  and also that (48) is identical to (40) for  $m + n = 1$  we see that assumption (30) produces similar distributions as assumption (29) but over an expanded range of  $m + n$ .

4. Applications

The solutions for the time-averaged salinity distributions in estuaries of generalized shapes derived in the previous section are now compared with observed distributions in eight estuaries. In arriving at these comparisons some inevitable approximations and assumptions were introduced; however,

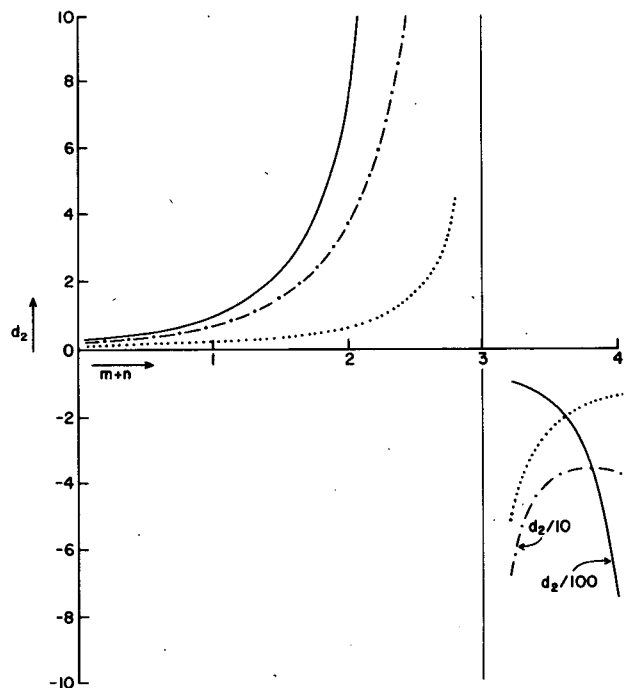


FIG. 6. Plots of  $d_2/(g/c_1^2 b_L)$ , where  $dx = d_2(dc/dx)^2$ — $a/x_1 = 0.001$ ; - - -  $a/x_1 = 0.1$ ; ····  $a/x_1 = 0.5$ .



the broad characteristics of both the theoretical and observed distributions should remain largely unaffected. The estuaries considered are (Table 1): the Waterways Experimental Station, Vicksburg (WES) flume, the Rotterdam waterway, the Hudson, and Potomac, the Delaware, the Bristol Channel, the Thames and the St. Lawrence. These were selected on the basis of readily available data and, with the exception of the WES flume, were all included in the earlier study of tidal response by Prandle and Rahman (1980). The WES results apply to a flume 0.23 m wide, 100 m long with a water depth of 0.15 m and with a "tidal" period of 600 s.

*a. Observational data*

The main parameters describing the observed distributions are shown in Table 1; the source of each

data set is indicated also. While the observed data might reasonably be assumed to represent cross-sectionally averaged values, some doubt about the effectiveness of the associated time-averaging must arise. The geometric parameters  $m$ ,  $n$  and  $\lambda$  were obtained from graphical representations of the actual estuarine dimensions (for details see Prandle and Rahman, 1980). The distance,  $x_1$  from the head at which the salinity is assumed to reach a constant value  $C_1$  is approximated by the value of  $x_0$  used previously to denote the mouth of each estuary. However, in the case of the Delaware and the Bristol Channel a constant salinity level is approximated within the estuaries and hence the observed values of  $x_1 (< x_0)$  are used. The values of  $B_1$  and  $H_1$  (the breadth and depth at  $x_1$ ), also were taken from the earlier study. The observed values of freshwater flow  $Q$  and the derived values for the diffusion co-

TABLE 1. (i) Estuarine dimensions. (ii) Salinity intrusion parameters.

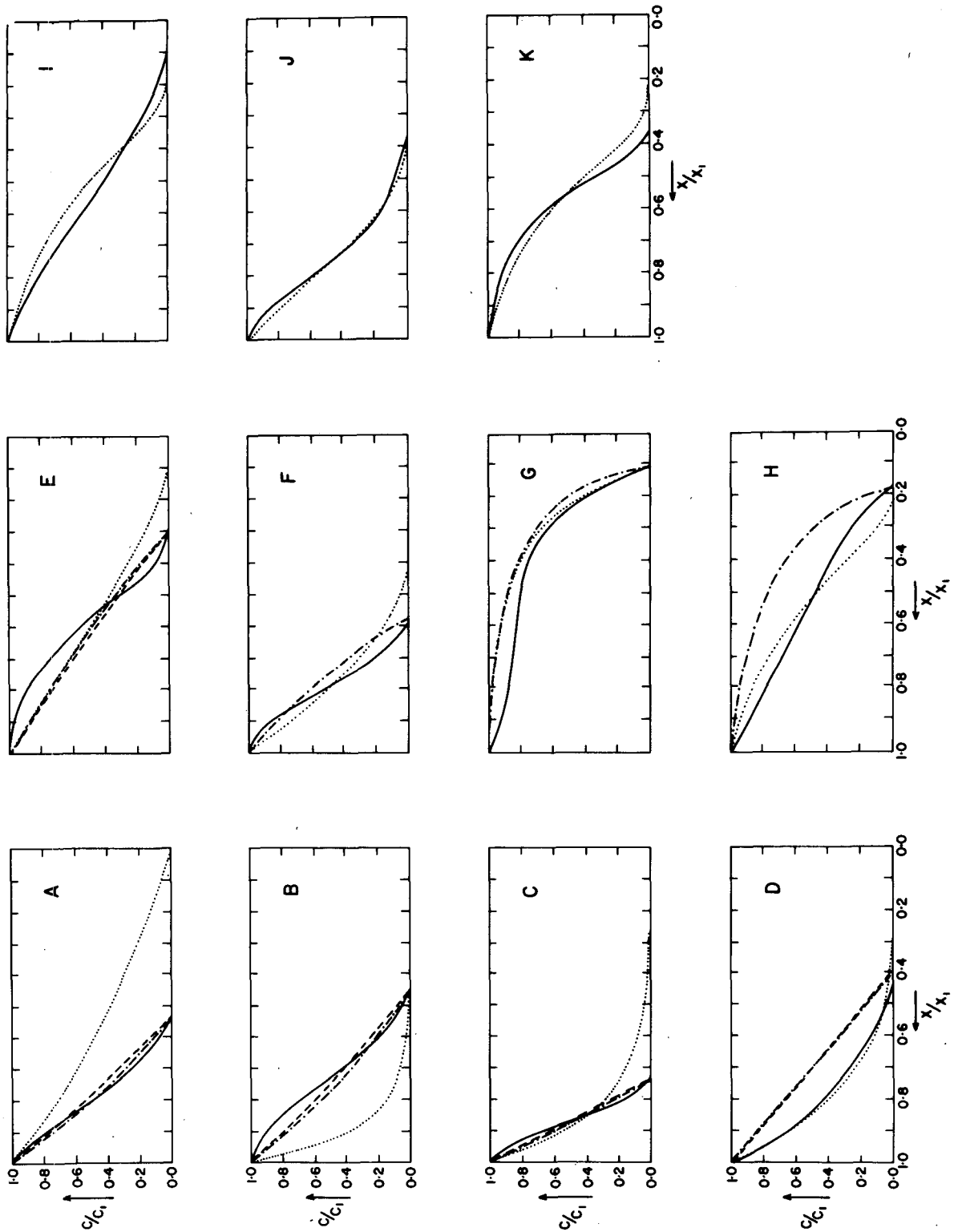
(i)	$m + n$	$x_1$	$\lambda$ (km)	$B_1$ (km)	$H_1$ (m)	Data source
WES flume	0	0.14	0.73	$0.23 \times 10^{-3}$	0.15	(a)
Rotterdam Waterway	0	0.19	505	0.41	13	(a)
Hudson	1.1	0.44	562	3.7	15	(a)
Potomac	1.4	0.37	495	18	10	(a)
Delaware	2.4	0.59	311	28	7	(a)
Bristol Channel	2.9	0.014	9815	20	25	(b)
Thames	3.0	0.078	1212	7	10	(d)
St. Lawrence	3.4	$1.2 \times 10^{-9}$	$3.6 \times 10^{11}$	48	300	(e)

(ii)	$Q$ ( $m^3 s^{-1}$ )	$V'$ ( $= \frac{U_1 X_1}{D}$ )	$D^*$ ( $m^2 s^{-1}$ )	$D$ observed ( $m^2 s^{-1}$ )	$D_1^*$ ( $m^2 s^{-1}$ )	$D_1$ model studies (c) ( $m^2 s^{-1}$ )	$D_2^*$ ( $m^2 s^{-1}$ )
WES flume	$0.21 \times 10^{-3}$ $2.12 \times 10^{-3}$	1 10	0.6		0.015 0.174	0.023 0.019	0.044 0.49
Rotterdam Waterway	960	6.3	2740		383	279	838
Hudson	99	4.0	111		134	157	126
Potomac	112	1.3	91		60	56	42
Delaware	141 300 467	2.5	112			108	640
Bristol Channel	80 480	0.08 0.48	270	54-174 124-535			4.6 19.8
Thames	19 210	0.47 2.1	87	53-84 338			
St. Lawrence	8500	0.5	510				

\* Values obtained from present study;  $x_1 = x_0$  (see Table 2, Prandle and Rahman) except for the Delaware and Bristol Channel. Values for the  $M_2$  constituent except for the W.E.S. flume where the period is 600 s.

- (a) Thatcher and Harleman (1972).
- (b) Bassindale (1943).
- (c) Bowden (1963).
- (d) Inglis and Allen (1957).
- (e) Partenscky and Louchard (1967).



efficients  $D$  and  $D_1$  defined in association with (28), (29) and (30) and also in (56) and (57) below, were taken from the sources shown in Table 1. These same sources were used to provide the observed distributions  $c(x)/c_2$  shown in Fig. 7. The precise value of  $Q$  for the observed distribution in the Delaware was uncertain and hence the middle of the three likely values shown was adopted.

*b. Theoretical distributions*

In calculating the theoretical distributions described by (40) [for  $d_x = d_1(dc/dx)$ ] and by (48) [for  $d_x = d_2(dc/dx)^2$ ] for any particular estuary, it is only necessary to determine the geometrical shape parameters  $m + n$  and the position of zero salinity  $x = a$ , i.e., the location of the upstream limit of saline intrusion. The determination of  $m + n$  was described in Section 4a. In the applications described here, the position of zero salinity is determined from the relevant observed salinity distribution.

In calculating the theoretical distributions described by (31) (for  $d_x = d$ ), in addition to the geometrical shape parameters  $m + n$ , it is necessary to specify both the value of the dispersion coefficient  $d$  and the position of zero salinity  $a$ . It was shown in Section 3a that 1) the salinity distributions can be greatly modified by adjusting the value of  $d$  alone and 2) imposing the condition  $c = 0$  at some intermediate position  $a$  has little effect if at that same position for the case of  $a = 0$ ,  $c$  is already close to zero. Thus, in determining theoretical distributions it seems sensible to adopt the value  $a = 0$  for all estuaries unless the particular conditions clearly indicate an alternative value. Moreover, by adopting the value  $a = 0$ , the change in salinity distribution under varying river discharges may be determined directly without the necessity of determining corresponding variations in the value of  $a$ .

In the results discussed in the following section the values of  $d$  were chosen by minimizing (in an approximate visual manner), the differences between the observed and theoretical distributions. The technique, described in Section 3a, of using the observed inflection point to make a first estimate for  $d$  proved extremely successful in this procedure.

*c. Comparison of observed and theoretical salinity distributions*

Fig. 7 shows a comparison of 11 distributions of observed and theoretical salinity distributions

in eight estuaries. Figs. 7a–7k are arranged in order of increasing values of  $m + n$ . In general, we see that the saline intrusion extends farther upstream as the value of  $m + n$  increases. This is in broad agreement with the results shown in Figs. 3 and 5 for  $d_x = d_1dc/dx$  and  $d_x = d_2(dc/dx)^2$ , respectively. However, to achieve this same result for  $dx = d$  it is necessary to decrease the value of  $V'$  as  $m + n$  increases. Although Table 1 shows that  $V'$  does decrease as  $m + n$  increases, it is difficult to relate this decrease to specific trends in the variables  $Q$ ,  $X_1$ ,  $B_1$ ,  $H_1$  or  $D$  (as previously indicated in Section 3a). Overall the general indication is that mixing tends to occur close to the head for those estuaries with a more rapidly truncating cross-sectional area (i.e., larger  $m + n$ ).

1) WES FLUME

The results from the WES flume may be considered separately from the real estuaries. The observed distributions are unusual in that the saline intrusion extends farther for the case of the higher flow rate ( $Q = 2.12 \times 10^{-3} \text{ m}^3 \text{ s}^{-1}$  compared with  $Q = 0.21 \times 10^{-3} \text{ m}^3 \text{ s}^{-1}$ ). This must be attributed to the larger tidal amplitude specified in the higher flow case, i.e., 0.030 m compared to 0.015 m. Since the present theoretical distributions take no account of tidal amplitudes it is hardly surprising to find that the results for  $d_x = d$  shown in Figs. 7a and 7b are considerably different from those observed. The results for  $d_x = d_1(dc/dx)$  and  $d_x = d_2(dc/dx)^2$  both agree well with observed distributions; however, this close agreement is a direct consequence of specifying the appropriate value for  $a$ .

The dimensional equivalents of  $d$ ,  $d_1$  and  $d_2$  were deduced as follows:

$$D = d \frac{\lambda^2}{P} = 1 / \left( \frac{u_1 x_1}{d} \right) = u_1 x_1 \frac{\lambda^2}{P}$$

$$= \frac{1}{V'} \times \frac{Q\lambda}{B_1 H_1} x_1, \tag{56}$$

similarly

$$D_1 = d_1 \frac{\lambda^2}{P} \quad \text{and} \quad D_2 = d_2 \frac{\lambda^2}{P} \tag{57}$$

Table 1 shows the values of these dimensional parameters. For the lower flow case the value of  $D_1$  found from the present study appears to be in reasonable agreement with the value used in the earlier modeling studies, whereas for the higher flow case the present value of  $D_1$  is larger by a factor of 10.

FIG. 7. Comparison of observed and theoretical time-averaged salinity distributions  $c(x)/c_1$  — observed;  $\cdots \cdots d_x = d$ ;  $----- d_x = d_1 dc/dx$ ;  $-\cdot-\cdot-\cdot d_x = d_2 (dc/dx)^2$ . (a) WES Flume,  $m + n = 0$ ,  $Q = 0.21 \times 10^{-3}$ ,  $V' = 1$ ; (b) WES Flume,  $m + n = 0$ ,  $Q = 2.12 \times 10^{-3}$ ,  $V' = 10$ ; (c) Rotterdam Waterway,  $m + n = 0$ ,  $Q = 960$ ,  $V' = 6.3$ ; (d) Hudson,  $m + n = 1.1$ ,  $Q = 99$ ,  $V' = 4.0$ ; (e) Potomac,  $m + n = 1.4$ ,  $Q = 112$ ,  $V' = 1.3$ ; (f) Delaware,  $m + n = 2.4$ ,  $Q = 300$ ,  $V' = 2.5$ ; (g) Bristol Channel,  $m + n = 2.9$ ,  $Q = 80$ ,  $V' = 0.08$ ; (h) Bristol Channel,  $m + n = 2.9$ ,  $Q = 480$ ,  $V' = 0.48$ ; (i) Thames,  $m + n = 3.0$ ,  $Q = 19$ ,  $V' = 0.47$ ; (j) Thames,  $m + n = 3.0$ ,  $Q = 210$ ,  $V' = 2.1$ ; (k) St. Lawrence,  $m + n = 3.4$ ,  $Q = 8500$ ,  $V' = 3.4$ .

TABLE 2. Values for the longitudinal dispersion coefficient  $D_x$  in estuaries.

Estuary	$D_x$ ( $\text{m}^2 \text{s}^{-1}$ )	Source
Severn	100–1000	Uncles and Radford (1980)
Thames	53–338	Bowden (1963)
Mersey	161–360	
Severn	54–535	
Columbia	5000	Dyer (1974)
James River	24	
Southampton Water	158	
Tay	50–300	

2)  $d_x = d$ 

Considering now the real estuaries from Figs. 7c to 7k we find the assumption  $d_x = d$  shows the best overall agreement. The Rotterdam Waterway shows an exceptionally high value for the dispersion coefficient  $D$ . The Waterway is an artificially channeled estuary only 400 m wide and is significantly stratified. This stratification may account for the large value of  $D$  as indicated by Bowden (1965) who suggested  $D$  might increase by an order of magnitude under such conditions. In the other six estuaries, the values of  $D$  lie in the range 50–500  $\text{m}^2 \text{s}^{-1}$ . This range is in close agreement both with values found in previous studies (as shown in Table 2) and with the values for  $D$  suggested by Smith (1980).

Figs. 7g and 7h show good agreement between observed and theoretical results for two significantly different flow conditions in the Bristol Channel and Figs. 7i and 7j show similarly good agreement for two flow conditions in the Thames. In both estuaries the two flow conditions approximate the extreme values of high and low river discharges and hence the theoretical models might be assumed to be reasonably accurate over the complete range of flow conditions. Moreover, for both estuaries the values of the dispersion coefficient  $D$  used in the models are shown in Table 2 to be in reasonable agreement with values obtained elsewhere. Thus, we may conclude that a one-dimensional, time-averaged model for salinity intrusion in estuaries employing a constant dispersion coefficient, in some cases, can provide a reliable and accurate simulation of actual conditions.

A number of dimensionless formulations for the longitudinal dispersion coefficient were examined. Eq. (56) employs the tidal period  $P$  and the longitudinal parameter  $\lambda$  to reduce  $D$  to the dimensionless parameter  $d$ . The following alternative parameters also were examined involving the breadth  $B_1$  and depth  $D_1$  at the mouth  $X_1$ :

$$d_B = \frac{DP}{\lambda B_1}, \quad (58)$$

$$d_H = \frac{DP}{\lambda H_1}. \quad (59)$$

However, the dimensionless parameters  $d$ ,  $d_B$  and  $d_H$  all exhibited a much wider range of values than the dimensional parameter  $D$ . This suggests that the dimensions of the mixing processes, in general, are not related to the gross estuarine parameters  $\lambda$ ,  $B_1$  or  $H_1$ .

This latter result contrasts with the significance of parameters such as the "stratification number" or "estuary number" introduced by Ippen and Harleman (1961) and Harleman and Ippen (1967), respectively. The greater usefulness of these latter dimensionless numbers probably derives from their use of parameters relating to the predominant tidal motions such as the tidal velocity  $U'$ . In the present approach, the dispersion process is related only to the freshwater flow while it has been shown (Chatwin, 1976) that this mechanism is insignificant in relation to other mixing processes. One technique for improving the present approach might be to relate the dispersion coefficient to  $U'$  or the tidal excursion as proposed by Arons and Stommel (1951).

3)  $d_x = d_1 dc/dx$  AND  $d_x = d_2 (dc/dx)^2$ 

Figs. 7c–7e show some agreement between observed results and those calculated for  $d_x = d_1 dc/dx$  but generally poorer than that found in Figs. 7a and 7b. Similarly, Figs. 7c–7h show some agreement between observed results and those calculated for  $d_x = d_2 (dc/dx)^2$  but, again, poorer than that found in Figs. 7a and 7b. Table 1 shows that the values for  $D_1$  corresponding to the calculated distributions shown in Figs. 7c, 7d and 7e [derived from (41) and (57)] are in good agreement with the values used in previous modeling studies. No comparable values exist against which the values for  $D_2$  shown in Table 1 might be compared.

Attempts were made to reduce these dimensional values for  $D_1$  and  $D_2$  to dimensionless forms as described by (57) and also in similar fashion to (58) and (59). However, it was again found that the dimensionless parameters were even more variable than their dimensional equivalents.

## 5. Concluding remarks

The earlier paper by Prandle and Rahman (1980) dealt with tidal response in estuaries of idealized shapes and established a classification system based on the length of the estuary and the value of the parameter  $\nu = (n + 1)/(2 - m)$ . The present investigation into saline intrusion in estuaries has not

revealed any single corresponding parameter of such fundamental significance. However, the theoretical solutions obtained showed the salinity distributions to be dependent on the distance along the estuary raised to some power involving the parameter  $m + n$ . This indicates that the variation in cross-sectional area is a fundamental parameter in determining the mixing pattern in an estuary.

In addition, the solutions obtained by assuming a constant longitudinal-dispersion coefficient  $D_x = D$  revealed the importance of the dimensionless parameter  $V' = U_1 X_1 / D$  with  $U_1$  representing the velocity of the freshwater flow at the position  $X_1$  where the estuary is effectively at oceanic salinity. By varying this parameter  $V'$  over the range 0.1–10.0, the pattern of saline distribution could be adjusted to produce mixing in the vicinity of either the head or the mouth or at any intermediate position. Comparison between observed and theoretical distributions in eight estuaries showed that the value of this parameter  $V'$  reduces as  $m + n$  increases, implying that mixing is likely to occur closer to the head in estuaries where the cross-sectional area truncates rapidly upstream.

These relationships between  $V'$  and salinity intrusion must be qualified by the neglect in the present paper of the effect of stratification. In general, intrusion will increase as stratification increases (Festa and Hansen, 1976; Bowden, 1965) and stratification increases as  $QH/U'B$  increases (Pritchard, 1955).

The values for  $D$  used in the present theoretical solutions lay in the range 50 to 500  $\text{m}^2 \text{s}^{-1}$  for six of the eight estuaries examined. (Attempts to express the dispersion coefficients in dimensionless forms involving estuarine length, breadth and depth produced a much wider range of values. It seems likely that more appropriate dimensionless forms could be obtained by using parameters relating to the predominant tidal motions such as tidal velocity or tidal excursion.) For those estuaries where corresponding values for  $D$  were available from previous studies, good agreement was shown with the present values. In addition, for two estuaries, the theoretical solutions were shown to be in good agreement with observed salinity distributions over a full range of river discharges, with the theoretical solutions employing a fixed value of  $D$  in each estuary.

Two alternative assumptions for the longitudinal-dispersion coefficient were examined, viz.,  $D_x = D_1(dc/dx)$  and  $D_x = D_2(dc/dx)^2$ . Again, the resulting theoretical salinity distributions were found to be in reasonable agreement with observed distributions and, in the case of  $D_x = D_1(dc/dx)$ , the values for  $D_1$  in most cases were in reasonable agreement with values found in previous studies. It is shown that these two forms for  $D_x$  are only

valid over a limited range of estuarine shapes and that the distributions which they produce are of a restricted form.

It is concluded that the solutions derived here (and elsewhere) for the one-dimensional time-averaged equation for salinity intrusion in estuaries, in some cases, can provide a reasonable simulation of actual conditions. In the case of  $D_x = D$ , the salinity distribution has been shown to be highly sensitive to the parameter  $V'$  and, consequently, to the value of  $D$ . Thus, models of this kind cannot be reliably applied 1) to estuaries where observational data are insufficient to determine  $D$  accurately or 2) to estuaries where some major change is proposed which might significantly alter the value of  $D$ . Similar qualifications apply to the use of the solutions obtained for  $D_x = D_1(dc/dx)$  and  $D_x = D_2(dc/dx)^2$ .

In nature, temporal and spatial variations in  $D_x$  must exist (Uncles and Radford, 1980; Hareman *et al.*, 1968) and the application of cross-sectional time-averaged solutions must be limited. Further progress must be in the direction of more sophisticated models able to incorporate spatial and temporal variations in density and momentum (Bowden and Hamilton, 1975; Blumberg, 1977).

*Acknowledgments.* Dr. M. Rahman (Technical University of Nova Scotia, Halifax, Canada) contributed significantly to the early development of this study during the time he and the author were colleagues at the Hydraulics Laboratory of the National Research Council, Ottawa, Canada.

#### REFERENCES

- Arons, A. B., and H. Stommel, 1951: A mixing-length theory of tidal flushing. *Trans. Amer. Geophys. Union*, **32**, 419–421.
- Bassindale, R., 1943: A comparison of the varying salinity conditions of the Tees and Severn estuaries. *J. Anim. Ecol.*, **12**, 1–10.
- Blumberg, A. F., 1977: Numerical model of estuarine circulation. *Proc. Amer. Soc. Civil Engrs. J. Hydro. Div.*, **103**, 295–310.
- Bowden, K. F., 1963: The mixing processes in a tidal estuary. *Int. J. Air. Water Pollut.*, **7**, 343–356.
- , 1965: Horizontal mixing in the sea due to a shearing current. *J. Fluid Mech.*, **21**, 83–95.
- , and P. Hamilton, 1975: Some experiments with a numerical model of circulation and mixing in a tidal estuary. *Est. Coast. Mar. Sci.*, **3**, 281–301.
- Chatwin, P. C., 1976: Some remarks on the maintenance of the salinity distribution in estuaries. *Est. Coast. Mar. Sci.*, **4**, 555–566.
- Curran, J. C., 1981: A finite-element model of pollution in the Clyde estuary. *Appl. Math. Model.*, **5**, 129–216.
- Dyer, K. R., 1974: Salt balance in stratified estuaries. *Est. Coastal Mar. Sci.*, **2**, 273–281.
- Festa, J. F., and D. V. Hansen, 1976: A two-dimensional numerical model of estuarine circulation: The effects of altering depth and river discharge. *Est. Coast. Mar. Sci.*, **4**, 309–323.

- Fischer, H. B., 1972: Mass transport mechanisms in partially stratified estuaries. *J. Fluid Mech.*, **53**, 4, 671–687.
- , 1976: Mixing and dispersion in estuaries. *Rev. Fluid Mech.*, **8**, 107–133.
- , E. J. List, R. C. Y. Koh, J. Imberger and N. H. Brooks, 1979: *Mixing in Inland and Coastal Waters*. Academic Press. 483 pp.
- Harleman, D. R. F., and A. T. Ippen, 1967: Two-dimensional aspects of salinity intrusion in estuaries. Tech. Bull. 13, Committee on Tidal Hydraulics, Corps of Engineers, U.S. Army, 39 pp.
- Harleman, D. R. F., C. H. Lee and L. C. Hall, 1968: Numerical studies of unsteady dispersion in estuaries. *Proc. Amer. Soc. Civil Engrs. J. Sanit. Eng. Div.*, **94**, 897–911.
- Holley, E. R., and D. R. F. Harleman, 1965: Dispersion of pollutants in estuary type flows. Rep. No. 74, Hydrodynamics Laboratory, MIT, 202 pp.
- , ——, and H. B. Fischer, 1970: Dispersion in homogeneous estuary flow. *Proc. Amer. Soc. Civ. Engrs. J. Hydro. Div.*, **96**, 1691–1709.
- Inglis, C. C., and F. H. Allen, 1957: The regime of the Thames Estuary as affected by currents, salinities and river flow. *Proc. Instrum. Civ. Engr.*, **7**, 827–878.
- Ippen, A. T., and D. R. F. Harleman, 1961: One-dimensional analysis of salinity intrusion in estuaries. Tech. Bull. 5, Committee on Tidal Hydraulics, Corps. of Engineers. U.S. Army, 52 pp.
- Ippen, A. T., Ed., 1966: *Estuary and Coastline Hydrodynamics*. McGraw-Hill, 744 pp.
- Kent, R., 1960: Diffusion in a sectionally homogeneous estuary. *Proc. Amer. Soc. Civ. Engrs. J. Sanit. Eng. Div.*, **86**, 15–48.
- Nihoul, J. C. J., and F. C. Ronday, 1975: The influence of the “tidal stress” on the residual circulation. Application to the Southern Bight of the North Sea. *Tellus*, **27**, 484–489.
- Partenscky, H. W., and L. Louchard, 1967: Etude sur la variation cyclique de la salinité moyenne dans l’estuaire du Saint Laurent. National Research Council, Ottawa, Canada. Unpublished Rep.
- Prandle, D., and M. Rahman, 1980: Tidal response in estuaries. *J. Phys. Oceanogr.*, **10**, 1552–1573.
- Pritchard, D. W., 1955: Estuarine circulation patterns. *Proc. Amer. Soc. Civ. Engrs.*, **81**, 717/1–717/11.
- Smith, R., 1976: Longitudinal dispersion of a buoyant contaminant in a shallow channel. *J. Fluid Mech.*, **78**, 677–688.
- , 1980: Buoyancy effects upon longitudinal dispersion in wide well-mixed estuaries. *Phil. Trans. Roy. Soc.*, **A296**, 467–496.
- Thatcher, M. L., and D. R. F. Harleman, 1972: A mathematical model for the prediction of unsteady salinity intrusion in estuaries. Report No. 144. Ralph M. Parsons Laboratory, Dept. Civil Eng., MIT, 232 pp.
- Uncles, R. J., and P. J. Radford, 1980: Seasonal and spring-neap tidal dependence of axial dispersion coefficients in the Severn—a wide, vertically mixed estuary. *J. Fluid Mech.*, **98**, 703–726.
- Williams, D. J. A., and J. R. West, 1973: A one-dimensional representation of mixing in the Tay Estuary. *Symposium on: Mathematical and Hydraulic Modelling of Estuarine Pollution*. Gameson, A. L. H., Ed., Water Pollution Research Tech. Pap. No. 13, Water Pollution Research Laboratory, Stevenage, Herts, England, 117–125.